

Anisotropic etching behaviour of gallium arsenide junctions

D. J. STIRLAND

Allen Clark Research Centre, The Plessey Company Limited, Caswell, Towcester, Northants, UK

A detailed study of the etching behaviour of junctions between gallium arsenide epitaxial layers and substrates of different carrier concentrations and carrier types has been made. Optical and scanning electron microscope examination of $\{110\}$ cleavage faces of (001) surface specimens has shown that high index facets are produced by the etchant used to delineate the junction. The facets are anisotropic on orthogonal $\{110\}$ faces: for example on a (110) face of an n^+ layer- n substrate configuration the facet extends from the junction into the substrate, whereas on the orthogonal (110) face the facet extends from the junction into the epitaxial layer. The widths of the facets (in $\langle 001 \rangle$ directions) increase linearly with etching time.

A simple model is presented which is able to account qualitatively for all the observed characteristics of the junction etching behaviour, and is based on the occurrence of differential etch rates at the epitaxial layer, junction, and substrate regions. A key assumption of the model is that the junction region is anisotropic in $[110]$ and $[\bar{1}10]$ directions, and reasons for this anisotropy are considered.

1. Introduction

The accurate determination of junction positions in epitaxial gallium arsenide layer structures is important both for fundamental investigations and in the design and fabrication of semiconductor devices. Three different techniques have been used for various elemental and compound semiconductors: infra-red interference [1], differential capacitance profiling [2], and optical observation of cleaved and etched junction cross-sections [3, 4]. When two different techniques have been used to compare junction positions for a series of gallium arsenide specimens [5], accuracies of $\sim \pm 10\%$ have been achieved for each method separately, but a valid comparison between the two sets of values depends on the parameter chosen to define the "true" junction position. For example, because the carrier concentration profile across an n^+/n interface is not a step-function, due to diffusion, some artificial position on the profile has to be chosen to specify the junction, e.g. the point at which the carrier concentration has become twice the background concentration. When a stain-type etchant is used after cleavage to indicate the "junction" position it is probable

that this position corresponds with the maximum variation in the carrier concentration with distance (i.e. maximum dn/dx) [6]. It will be shown in Section 2.2 that a demarcation line between regions apparently corresponding with layer and substrate is observed on $\{110\}$ faces after cleavage alone. All subsequent references to junction position will signify the position of this demarcation line which is believed to be the "metallurgical" junction, i.e. the original substrate surface position before epitaxial layer growth.

The cleave-and-etch method appears to be the most direct technique for junction location, although a disadvantage is that part of the specimen is destroyed. An (001) gallium arsenide slice overlaid with one or more epitaxial layers is cleaved along $\langle 110 \rangle$ to expose a $\{110\}$ face orthogonal to the (001) slice surface. A brief immersion in a suitable etchant produces a line, or several lines, at the junction(s), which can be seen by low power optical examination. Abrahams and Buicchi [7] have examined gallium arsenide p - n junctions in injection lasers on both (110) and $(\bar{1}10)$ cleavage faces after etching with the AB

TABLE I

	Specimen identification					
	A	B	C	D	E	F
Layer growth method	VPE	VPE	VPE	VPE	VPE	VPE
Layer/substrate dopants	S/Sn	S/Sn	S/Si	Sn/Sn	S/Cd	S/Cr
Layer/substrate carrier concn. (cm ⁻³)	7.0 × 10 ¹⁷ / 3.0 × 10 ¹⁶	2.5 × 10 ¹⁵ / 4.0 × 10 ¹⁷	6.5 × 10 ¹⁵ / 1.0 × 10 ¹⁸	1.5 × 10 ¹⁵ / 3.7 × 10 ¹⁷	1.9 × 10 ¹⁵ / 2.0 × 10 ¹⁷	2.4 × 10 ¹⁵ / high resistivity ~10 ⁸ Ω cm n/semi-insulating
Layer/substrate carrier types	n ⁺ /n	n/n ⁺	n/n ⁺	n/n ⁺	n/p ⁺	n/semi-insulating
Layer thickness (μm)	312	7.5	0.65 ± 0.05	65	82	17.8

etch [8], and have reported that a band, rather than a line, is formed in the vicinity of the junction. The purpose of this paper is to describe some of the characteristics of this band, which will be referred to as the AB etch band; in particular it will be shown that the position of the band differs on (110) and $(\bar{1}\bar{1}0)$ orthogonal and contiguous cleavage faces.

2. Experimental

2.1. Specimen preparation

A number of vapour grown (VPE) and liquid grown (LPE) epitaxial layer-substrate combinations of different dopants, carrier concentrations, and thicknesses have been examined. The details are listed in Table I. All specimens were of (001) surface orientation.

It will be seen later that it was necessary to examine contiguous cleavage faces. To do this, four cleavages were made on each sample, so that two nominally undamaged [001] edges bounding $(\bar{1}\bar{1}0)/(\bar{1}\bar{1}0)$ and (110)/ $(\bar{1}\bar{1}0)$ cleavage faces were formed, as shown in Fig. 1.

The thinner layer specimens were waxed before cleavage, to prevent attack of the {001} surfaces by the AB etch. Cleaved specimens, ~1 cm × 1 cm in area, were etched in 10 ml of freshly prepared solution, at room temperature and with continuous agitation [8]. They were then either mounted on a $(\bar{1}\bar{1}0)$ face for optical examination of the (110) face, followed by remounting on (110) for examination of $(\bar{1}\bar{1}0)$, or were fixed with [010] normal to a scanning electron microscope (SEM) specimen stud so that the (110) and $(\bar{1}\bar{1}0)$ faces could be examined simultaneously.

Some specimens were given a "conventional" cleave-and-etch treatment (i.e. immersion for 10 to 30 sec in HF:HNO₃:H₂O, 1:3:4) to

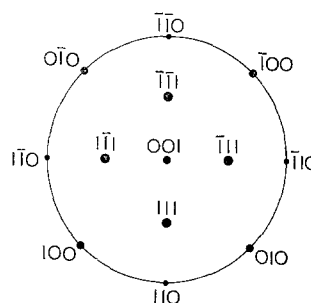
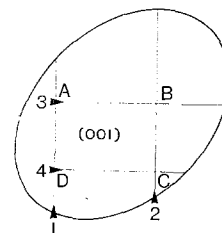


Figure 1 Preparation of specimen by cleavage, together with stereographic projection of gallium arsenide sample. 1-4: order of cleavage, to produce $\langle 110 \rangle$ sided specimen, with B and C [001] damage-free edges.

determine the junction position. In most cases this position could be seen using interference contrast microscopy, without any etch treatment after cleavage. The junction position relative to the AB etch bands was determined by viewing areas which had been partially masked after a conventional junction etch (CJE) but before a subsequent AB etch (see following section).

2.2. Experimental results

2.1.1. Observations of etched junctions

(Unless otherwise indicated, all illustrations are

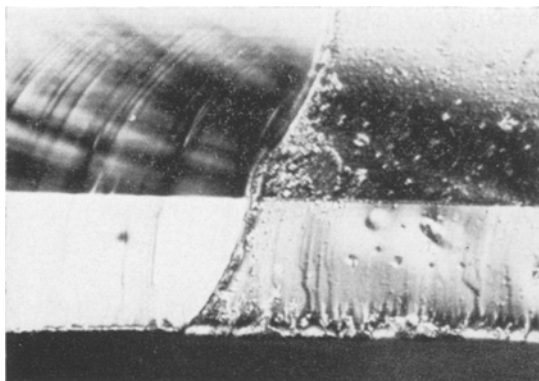


Figure 2 (110) cleavage face of specimen A. LHS unetched, RHS etched 30 sec in HF/HNO₃/H₂O. $\times 200$.

interference contrast (Nomarski) micrographs. The epitaxial layer is always shown above the substrate.)

Fig. 2 shows the correspondence between an as-cleaved, unetched, junction and a conventionally etched junction (CEJ) of specimen A; the curved line marks the right hand boundary of the plastic film used to protect the area on the left side during the junction etch treatment. Since this boundary is visible after removal of the plastic film it is apparent that the junction etch has removed material both from the layer and substrate, as well as the junction. A 4 min etch in the AB solution removes considerably more material, as can be seen in Fig. 3. This shows the relation between the CEJ and the AB etch band position as revealed by optical examin-

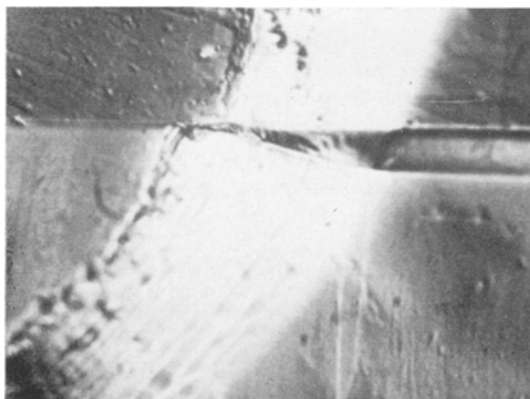


Figure 3 (110) cleavage face of specimen A. LHS etched 30 sec in HF/HNO₃/H₂O, RHS etched 4 min in AB etch. $\times 550$.

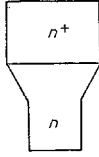
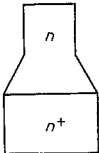
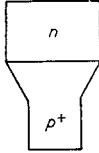
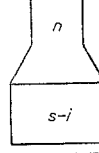

ation of the (110) cleavage face. The AB etch band of Fig. 3 is out-of-focus: the AB etch treatment has removed $\sim 30 \mu\text{m}$ of gallium arsenide from the right hand side of the specimen.

These micrographs indicate several characteristics of the etching behaviour of all the junctions which have been examined. The CJE does not produce a single line, i.e. a step, at the junction. Fig. 2 shows that the etched junction appears as two lines, more clearly resolved as a thin band $\sim 2.7 \mu\text{m}$ wide on Fig. 3. Fig. 2 also shows that the upper boundary of the CEJ is continuous with the boundary delineated by the cleavage alone, that is, the lower CEJ boundary lies in the substrate. The AB etch treatment has in effect expanded the CEJ band width from the cleavage junction; on Fig. 3 the upper boundary of the AB etch band coincides with the upper boundary of the CEJ, whereas the lower boundary of the AB etch band is $\sim 21 \mu\text{m}$ below in the substrate. Similar observations have indicated that a converse effect occurs on the ($\bar{1}10$) cleavage face. The lower edge of the CEJ is continuous with the lower boundary of the AB etch band, and the upper boundaries of both bands are located in the layer region.

2.2.2. Crystallographic nomenclature

It is necessary at this stage to define the crystallographic notation used in the following (and previous) sections. The choice of a specific plane such as (110) to represent one cleavage face of an (001) surface gallium arsenide specimen is arbitrary, although, the choice having been made, all other specific planes are fixed. Because the III-V compounds, with zinc-blende structure, exhibit polarity along $\langle 111 \rangle$ directions, a further restriction has to be imposed for a unique representation of a specific plane or direction. The conventional nomenclature [9] will be adopted, that is (111), ($1\bar{1}\bar{1}$), ($\bar{1}\bar{1}1$) and ($\bar{1}1\bar{1}$) planes will be designated as Ga-rich planes, or A planes, and ($\bar{1}\bar{1}\bar{1}$), ($\bar{1}\bar{1}1$) ($11\bar{1}$) and ($1\bar{1}1$) planes will therefore be As-rich, or B, planes. The (110) plane will then be specified as that cleavage face on which the *upper* boundary of the AB etch band (or the CEJ) coincides with the junction line revealed by cleavage alone, for an epitaxial layer lying *above* a substrate, and for the system in which the substrate etches faster than the layer (see Section 2.2.5.). This specification will give a consistent nomenclature; the absolute validity is discussed in Section 3.2.2.

TABLE II Summary of experimental details and measurements (see text for full description)

Specimen	1. AB etch time (min at room temperature)	2. AB etch band width (μm)			3. AB etch band inclination from $\langle 001 \rangle$		4. Layer/ substrate con- figuration after AB etch	5. Figure no.
		(110)	($\bar{1}10$)	{110}†	(110)	($\bar{1}10$)		
A	1.75	—	—	8.2				3
	3.0	—	—	17.4				
	4.0	16.5	14.0	—				
	5.0	—	—	23.0				
	8.0	—	—	37.0				
	9.0	71.4	68.3	—	$7.0^\circ \pm 1.0^\circ$	$6.5^\circ \pm 1.0^\circ$		
	12.0	59.5	57.0	—	$7.0^\circ \pm 1.0^\circ$	$6.0^\circ \pm 1.0^\circ$		
	1.0*	23.2	29.5	—				
B	0.67	1.9	2.1	—				
C	2.5	3.9	0.5	—				9
			± 0.1					
D	4.5‡	20.6	21.8	—	$5.0^\circ \pm 1.0^\circ$	$5.0^\circ \pm 1.0^\circ$		
E	4.5‡	18.4	18.4	—	$5.5^\circ \pm 1.0^\circ$	—		
F	3.0	8.9	9.7	—				

Notes: †The {110} readings were taken from one (non-specific) cleavage face.

*Etched at 65°C .

‡Samples etched together.

2.2.3. AB etch band width

Table II, column 2, shows sets of measurements of the AB etch band widths on (110) and ($\bar{1}10$) cleavage faces from specimen A, after different etching times. Previous (unpublished) experiments on the measurement of AB etching rates on (001) gallium arsenide surfaces have shown that the reproducibility of etching rates is limited to $\sim \pm 20\%$, under the most favourable conditions. For this accuracy, constant agitation of freshly prepared etch is necessary, and reproducibility worsens for short (< 2 min) and long (> 10 min) etch times. Within these limitations, it is concluded that the AB etch band widths are the same on contiguous cleavage faces for constant etching times, and that the

band width increases linearly with increasing etching time, for specimen A, at $\sim 4.7 \mu\text{m min}^{-1}$.

The single experiment performed at 65°C confirms the observation of Abrahams and Buiocchi [8] that AB etch rates at this temperature are approximately four times greater than at room temperature.

2.2.4. Anisotropy of AB etch bands

The observations of Section 2.2.1. have shown that the AB etch band does not appear in the same position on contiguous {110} faces. This is clearly illustrated by SEM examination of (110) and ($\bar{1}10$) faces simultaneously, as shown in Fig. 4, of another specimen A sample, etched for 12 min in the AB etchant.



Figure 4 (110) and $(\bar{1}\bar{1}0)$ cleavage faces of specimen A viewed along $[0\bar{1}0]$. Etched 12 min in AB etch. SEM micrograph, $\times 130$.

The higher magnification view of Fig. 5 shows that the upper boundary of the (110) junction band and the lower boundary of the $(\bar{1}\bar{1}0)$ junction band are continuous (to within $\pm 0.1 \mu\text{m}$), which is to be expected if they are located at the "cleavage junction", as discussed in Section 2.2.1.

By rotation of the SEM specimen in the microscope, silhouette-type profiles of the (110) and $(\bar{1}\bar{1}0)$ faces seen along $[1\bar{1}0]$ and $[\bar{1}\bar{1}0]$ directions, respectively, were obtained. These showed that the AB etch bands are

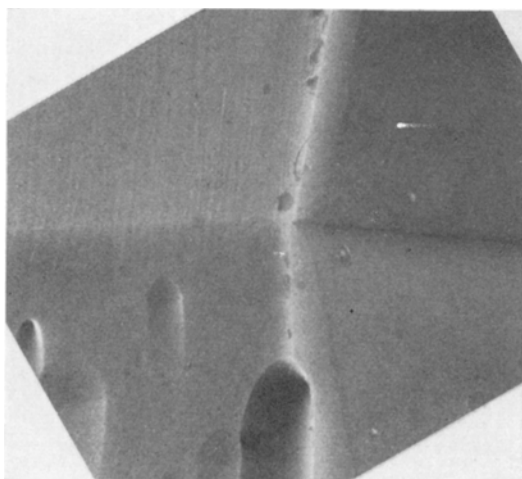


Figure 5 (110) and $(\bar{1}\bar{1}0)$ cleavage faces of specimen A at junction region, view along $\sim[0\bar{1}0]$ at junction region. Etched 12 min in AB etch SEM micrograph, $\times 2000$.

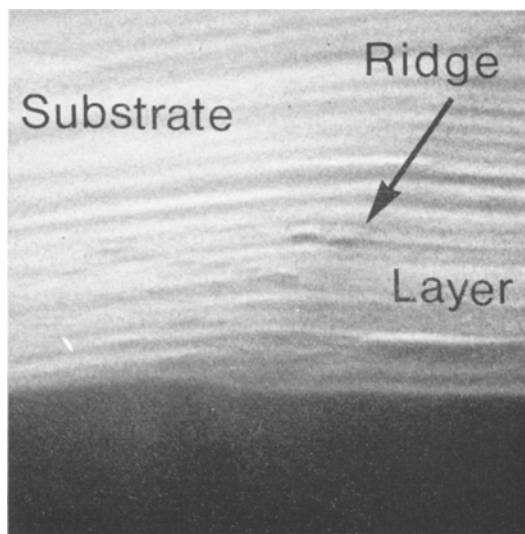


Figure 6 (110) cleavage face of specimen A, view approximately along $[1\bar{1}0]$. Etched 12 min in AB etch. SEM micrograph, $\times 20000$.

essentially facets, bounded on one side by the junction. The inclination of the (110) face facet is $7.0^\circ \pm 1.0^\circ$ from $[001]$ towards $[110]$; the inclination of the $(\bar{1}\bar{1}0)$ face facet is $6.0^\circ \pm 1.0^\circ$ from $[001]$ towards $[\bar{1}\bar{1}0]$. From SEM and optical profile micrographs (see Section 2.2.5) several values of the etch facet angles were measured for different layer-substrate combinations: they are given in column 3 of Table II. Figs. 6 and 7 are higher magnification views, at near glancing angle, of the two junction regions. They show that the (110) junction is slightly carinated, or ridged, whereas the $(\bar{1}\bar{1}0)$ junction is grooved.

2.2.5. The layer-substrate configuration after AB etch treatment

Fig. 8 is an exaggerated representation of the shape which is found to result from an AB etch treatment of a $\{110\}$ sided, $\{001\}$ faced rectangular n^+/n sample (e.g. similar to specimen A). This was deduced from optical and SEM examinations such as Figs. 4 to 7. The slopes of the junction facets have been increased to $\sim 20^\circ$ for clarity. The diagram shows that the substrate has been etched more than the layer; thus for specimen A the etch rate of an (n)tin-doped substrate (3×10^{16} carriers cm^{-3}) is greater than that of the (n^+)sulphur doped epitaxial layer (7×10^{17} carriers cm^{-3}).

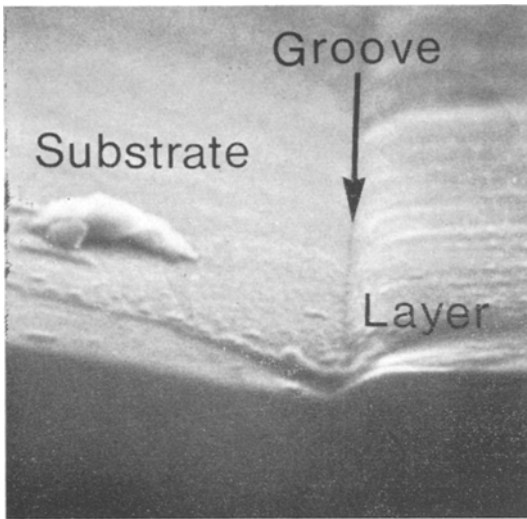


Figure 7 $(\bar{1}10)$ cleavage face of specimen A, view approximately along $[\bar{1}\bar{1}0]$. Etched 12 min in AB etch. SEM micrograph, $\times 20\ 000$.

Fig. 9 shows a pair of optical micrographs of (110) and $(\bar{1}10)$ cleavage faces, AB etched for $4\frac{1}{2}$ min, of specimen D. The profile of the (110) etch facet can be seen (PQ) on the $(\bar{1}10)$ face micrograph, and the $(\bar{1}10)$ facet profile (at RS) on the (110) face. It is clear that for this sample the (n) tin-doped layer (1.5×10^{15} carriers cm^{-3}) has been etched more than the (n^+) tin-doped substrate (3.7×10^{17} carriers cm^{-3}), so

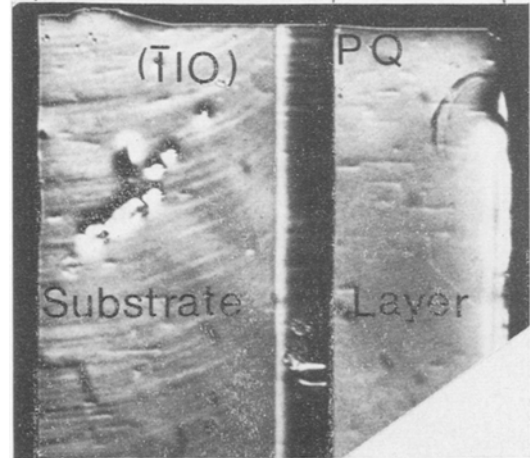
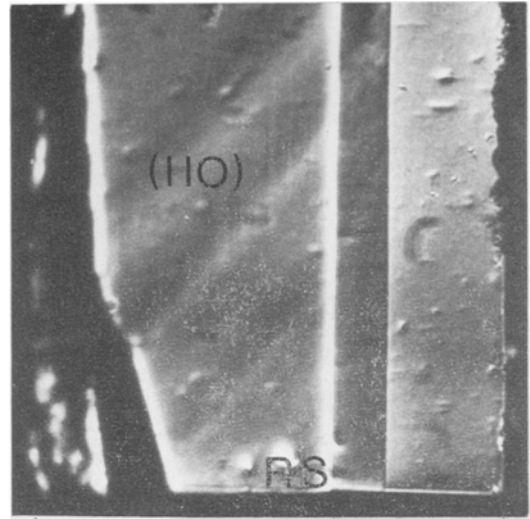


Figure 9 (110) and $(\bar{1}10)$ cleavage faces of specimen D, correctly aligned along common $[001]$ edge. Etched $4\frac{1}{2}$ min in AB etc. $\times 315$.

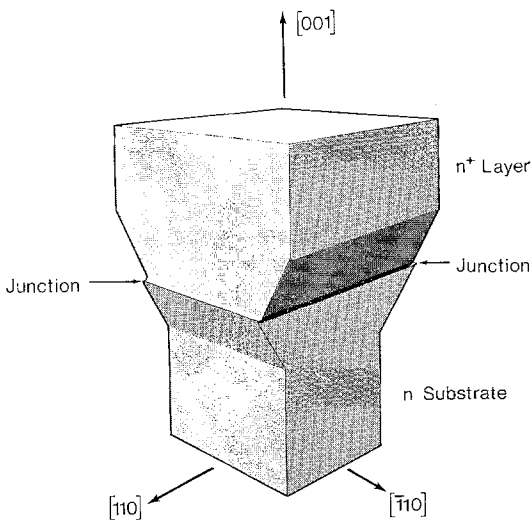


Figure 8 Exaggerated representation of n^+/n layer-substrate specimen after AB etching of $\{110\}$ cleavage faces.

that an equivalent representation of Fig. 8 in this case would be obtained by turning the diagram upside down.

Provided that sharp undamaged $[001]$ edges could be formed by cleavage between (110) and $(\bar{1}10)$ faces as shown in Fig. 1, it was possible to use this profile examination method to determine relative etch rates for a range of layer-substrate combinations. These results are given in diagrammatic form in column 4 of Table II.

If it is assumed that the etch rate differences are solely governed by carrier concentration differences, the following sequences are deduced

$$R_{p^+} > R_n > R_{n^+} : \text{for } p^+ = 2 \times 10^{17} \text{ (carriers cm}^{-3}\text{)}$$

$$n = 1.5 \times 10^{15} \text{ to } 3 \times 10^{16}$$

$$n^+ = 3.7 \times 10^{17} \text{ to } 7 \times 10^{17}$$

and

$$R_n > R_{(\text{semi-insulating})} : \text{for } n = 2.4 \times 10^{15}$$

where R_c = etch rate in $\langle 110 \rangle$ direction for gallium arsenide of carrier type c .

3. Discussion

3.1. Summary of experimental observations

Any explanation of the AB junction etching behaviour has to account for five experimental observations summarised as follows:

1. An AB etch treatment of (110) and adjacent $(\bar{1}\bar{1}0)$ cleavage faces for a layer-substrate structure with different carrier concentrations produces etch band "facets" at the junction.

2. The (110) etch band facet lies in the substrate and is bounded by the junction; the $(\bar{1}\bar{1}0)$ etch band facet lies in the layer and is bounded by the junction, for an n^+ layer- n substrate configuration.

3. The (110) cleavage face is carinated at the junction; the $(\bar{1}\bar{1}0)$ face is grooved at the junction, for an n^+ layer- n substrate configuration.

4. The widths of the etch band facets are approximately equal (measured parallel to $\{110\}$ faces) for constant etch times, on adjacent $\{110\}$ faces, and increase linearly with increasing etching time.

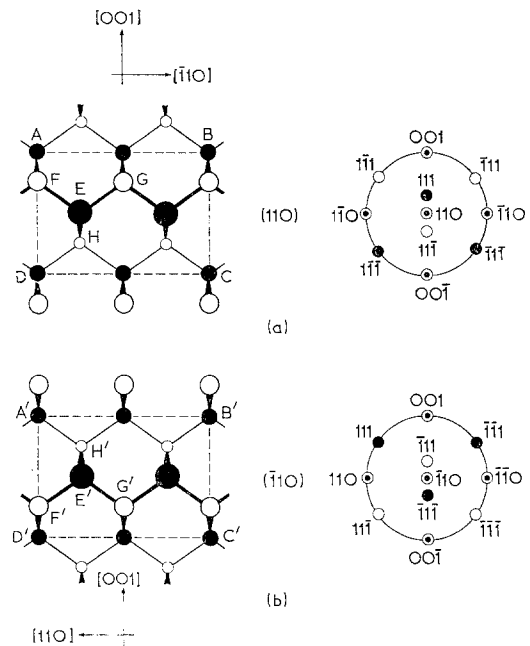
5. The inclinations of the facets from [001] appear to be constant (within experimental limits) for varied etch times, with a value of $\sim 6.0^\circ \pm 1.0^\circ$ for specimen A, and similar values for the other measured samples. See Table II, column 3, for these results.

3.2. Proposed explanation for junction etching anisotropy

The mechanism suggested here will deal specifically with the configurations of the etch band facets which result from an AB etch treatment of specimen A, i.e. an n^+ (sulphur doped) layer on an n (tin doped) substrate, although a qualitatively similar explanation will hold for other layer-substrate combinations.

3.2.1. Crystallographic structures of (110) and $(\bar{1}\bar{1}0)$ gallium arsenide planes

Figs. 10a and b show the atomic configurations of (110) and $(\bar{1}\bar{1}0)$ planes, together with their stereographic projections, for which the filled (\bullet) and open (\circ) symbols represent Ga and As rich poles; the \odot symbol represents a non-polar pole. This symbolism must not be confused with the conventional crystallographic notation of filled and open circles to represent poles in the upper and lower hemispheres. All the poles in Fig. 10 are in the upper hemisphere. An important factor to be recognized is that any direction $[hhl]$ or $[hh\bar{l}]$ lying on the $1\bar{1}0$ zone of Fig. 10a (excluding [001], [110] and $[00\bar{1}]$) will be a "partially polar" direction, although clearly the $[111]$ and $[11\bar{1}]$ directions represent maximum (\bullet) polarity and maximum (\circ) polarity. Similarly, any $[\bar{h}hl]$ or $[\bar{h}h\bar{l}]$ direction, excluding [001], $[\bar{1}\bar{1}0]$ and $[00\bar{1}]$, lying on the 110 zone of Fig. 10b will be "partially-polar", with opposite "partial-polarity" to the $[hhl]$ or $[hh\bar{l}]$ directions. The (110) and $(\bar{1}\bar{1}0)$ planes



- \bullet Ga in planes ABCD, A'B'C'D'
- \circ As in planes ABCD, A'B'C'D'
- \bullet Ga $\frac{1}{4}a_0$ (110) above ABCD, A'B'C'D'
- \circ As $\frac{1}{4}a_0$ (110) above ABCD, A'B'C'D'

Figure 10 Atomic structures and stereographic projections of (a) (110) cleavage face, and (b) $(\bar{1}\bar{1}0)$ cleavage face. See text for full explanation.

contain equal numbers of Ga and As atoms within each plane, so that $\langle 110 \rangle$ directions exhibit no polarity. If $\{110\}$ surfaces are attacked, the (110) etch rate should be equal to the $(\bar{1}10)$ etch rate. Gatos and Levine [10] have shown that anisotropic etch figures are formed on $\{110\}$ and $\{100\}$ surfaces of III-V compounds which appears to conflict with this statement. However, this was shown to be due to the development of $\{111\}$ facets at etch figures produced by the preferential attack of defects intersected by the $\{110\}$ and $\{100\}$ surfaces: because polarity differences exist in the various $\langle 111 \rangle$ directions of the etched facets, an anisotropy in the shape of the etch figures develops. For defect-free $\{110\}$ surfaces the etch rates should be constant.

3.2.2. Junction anisotropy after etching

The experimental results shown in diagrammatic form in Fig. 8 suggest that at least three different etch rates have been operative at each $\{110\}$ cleavage face: at the n^+ region, at the n region, and at the junction itself. In the following, we shall treat the etch rates as vector quantities; thus $R[\bar{1}\bar{1}0]n^+$ will represent the etch rate R (in $\mu\text{m min}^{-1}$) operative in a $[\bar{1}\bar{1}0]$ direction (i.e. etching *into* the (110) face) in n^+ material.

$RJ[\bar{1}\bar{1}0]$ will represent the junction etch rate for the junction appearing on the (110) face. For the (110) face the three rates are therefore $R[\bar{1}\bar{1}0]n^+$, $RJ[\bar{1}\bar{1}0]$, and $R[\bar{1}\bar{1}0]n$ and for the $(\bar{1}10)$ face they are $R[\bar{1}\bar{1}0]n^+$, $RJ[\bar{1}\bar{1}0]$, and $R[\bar{1}\bar{1}0]n$. This notation can be simplified, because the comments in Section 3.2.1 have shown that $R[\bar{1}\bar{1}0]n^+ = R[1\bar{1}0]n^+ = R_{n^+}$ say and similarly $R[\bar{1}\bar{1}0]n = R[1\bar{1}0]n = R_n$.

Fig. 9 also indicates that

$$R_{n^+} < R_n \quad (1)$$

Since the (110) face after etching shows a slight ridge at the junction, whereas the $(\bar{1}10)$ face has a groove at the junction, it is assumed that

$$RJ[\bar{1}\bar{1}0] < RJ[1\bar{1}0] \quad (2)$$

This is discussed fully in Section 3.3.

Fig. 11a indicates the various etch vectors for both $\{110\}$ cleavage faces; the two orthogonal faces are shown with a rotation of π for ease of presentation. $X_1Y_1Z_1$ and $X_1'Y_1Z_1'$ are points entirely within the n^+ , junction, and n regions respectively for both $\{110\}$ faces. In the absence of other directional etching, these points will become $X_2Y_2Z_2$ and $X_2'Y_2'Z_2'$ after some short

but finite etching time, as shown in Fig. 11b. It is assumed that plane facets X_2Y_2 , Y_2Z_2 etc. join these points, with inclinations ϕ_{1-4} as indicated. It will be seen later that the exact configuration postulated for these facets is unimportant, in fact the same final configuration will be achieved if curved surfaces are chosen, but it is easier to consider the simplified form of Fig. 11b at this stage.

The indices of the facets X_2Y_2 etc. will be represented by:

$$\begin{aligned} X_2Y_2 &= (h_1h_1l_1)C \\ Y_2Z_2 &= (h_2h_2l_2)D \\ X_2'Y_2' &= (\bar{h}_3\bar{h}_3\bar{l}_3)C \\ Y_2'Z_2' &= (\bar{h}_4\bar{h}_4\bar{l}_4)D \end{aligned}$$

where symbols C and D indicate the "partial-polarity" of the facets, as discussed in Section 3.2.1. The notation is consistent with the stereo-projections of Fig. 10. The final procedure is to consider how these four facets may change with further etching treatment. It is apparent that extra "etch vectors" in directions normal to the facets have to be considered, and the notation used will be e.g.: $R_1(C)n^+$ to represent the etch rate of facet X_2Y_2 (slope ϕ_1) in the partially-polar (C) direction in n^+ material; $R_2(D)n$ to represent the etch rate of facet Y_2Z_2 (slope ϕ_2) in the partially-polar (D) direction in n material; etc. Fig. 11b shows these additional etching directions, for both $\{110\}$ surfaces; the etch vectors of Fig. 11a should also be present on this diagram, but they have been omitted for clarity.

Crystal facets which jut out into an etchant will be attacked in such a way that the *slowest* etching facets are eventually eliminated. The converse is true for etching of re-entrant facets: in this case the *fastest* etching facets are eliminated [10]. Thus for the (110) surface, Fig. 11b, provided that

$$R_1(C)n^+ > R_{n^+} \quad (3)$$

and

$$R_2(D)n < R_n \quad (4)$$

facet X_2Y_2 will be eliminated, and facet Y_2Z_2 will enlarge (i.e. the position of Z_2 will move further from the fixed Y_2).

Similarly, for the $(\bar{1}10)$ surface, provided that

$$R_3(C)n^+ > R_{n^+} \quad (5)$$

and

$$R_4(D)n < R_n \quad (6)$$

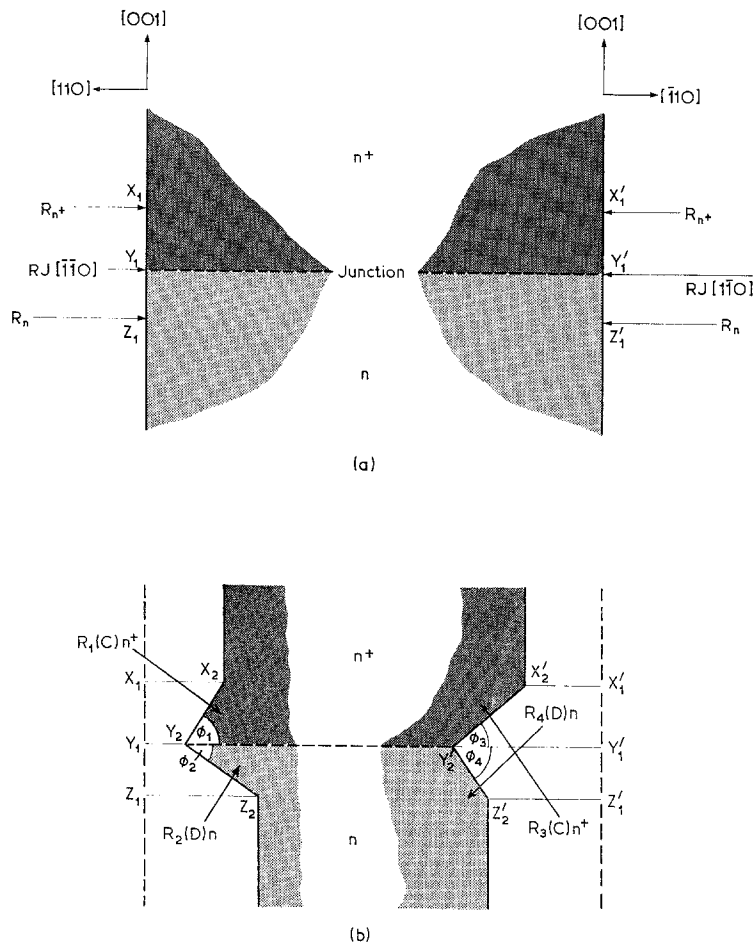


Figure 11 (a) Etch rates at (110) and (1 $\bar{1}$ 0) junction regions, (b) expected configuration after etch attack.

facet $X'_2Y'_2$ will enlarge, and facet $Y'_2Z'_2$ will disappear.

Experimentally, the inclinations of facets Y_2Z_2 and $X'_2Y'_2$ have been measured (column 3, Table II) and are equal in magnitude, within the accuracy possible. Thus $\phi_2 = \phi_3$. ϕ_1 and ϕ_4 cannot be measured, of course, because they are not observed. However, it is a reasonable assumption that $\phi_1 = \phi_2 = \phi_3 = \phi_4$.

This reduces the inequalities of Equations 3 to 6 to two inequalities:

$$R(C)n^+ > R_{n^+} \quad (7)$$

and

$$R(D)n < R_n \quad (8)$$

There are thus four relationships which, if obeyed, result in the observed facet appearances on orthogonal {110} faces (of specimen A): Equations 7, 8, 1 and 2. It can be inferred from

Equation 7 that $R(C)n > R_n$, and from Equation 8 that $R(D)n^+ < R_{n^+}$, since the ratios of etch rates in different directions are unlikely to depend on parameters other than the crystallographic orientations (polarities) in different directions. Therefore, Equations 7 and 8 can be combined to give:

$$R(C) > R > R(D) \text{ for } n \text{ or } n^+ \quad (9)$$

A set of conditions has been established which will result in the observed experimental etch band configurations. One ambiguity remains: is the selection of [111] Ga and $[\bar{1}\bar{1}\bar{1}]$ As directions correct? It is apparent that an interchange of Ga(●) for As(O) throughout will still result in a self-consistent explanation.

This ambiguity can be eliminated by determination of a correct specific $\langle 111 \rangle$ direction. Huber and Champier [11] have described

elongated etch features ("boat pits") produced by an AB etch of (001) gallium arsenide surfaces, which lie in *one* $\langle 110 \rangle$ direction only. These are analogous to the etch figures reported by Gatos and Levine [10] on $\{100\}$ and $\{110\}$ surfaces, and their directional anisotropy derives from exposure of $\{111\}$ (polar) facets at etched defects in the surface. Thus the elongation direction will specify a particular $\langle 110 \rangle$ direction provided it is known which $\{111\}$ faces are attacked fastest. Observation of (001) and $\{110\}$ faces after etching can thus enable a correct designation of specific $\{110\}$ planes to be made. Abrahams and Buiocchi [8] have already shown that the $[111]$ Ga etch rate is greater than the $[\bar{1}\bar{1}\bar{1}]$ As etch rate. Using this information, and by observation that the "boat pits" on the (001) layer surfaces were elongated along $[110]$ directions, it was shown that the nomenclature adopted here was correct, for specimen A.

3.3. Implications of the proposed explanation

It is evident that the explanation given in the previous section is able to account qualitatively for all the experimental observations summarised in Section 3.1 and, therefore, it is necessary to critically consider the stated or implied postulates on which this explanation is based. These are:

1. $\{110\}$ surfaces of different carrier concentrations etch at different rates;
2. junction etch band facets consist of high index planes, with equal and opposite angular inclinations about $[001]$;
3. a partially polar (hhl) surface etches at a different rate than a partially polar ($h\bar{h}\bar{l}$) surface;
4. the (110) junction etches slower in the $[\bar{1}\bar{1}0]$ direction than the same $(\bar{1}10)$ junction does in the $[1\bar{1}0]$ direction.

1. This is the basis of cleave-and-stain methods of determining junction positions in general. No attempt has been made yet to compare the effects of different dopant combinations with similar carrier concentration combinations, or the effects of markedly different carrier concentrations, on the appearances of the junction etch band facets. However, since the parameters which determine ϕ (and hence the indices of facets Y_2Z_2 and $X_2'Y_2'$) involve Equation 1, variations in ϕ should be achievable in principle.

2. This is an experimental observation rather

than an assumption. However, the proposed explanation indicates that plane facets should occur with prolonged etching, regardless of the initial configuration of the junction region shown in Fig. 11b. For example, if X_2Y_2 and Y_2Z_2 are curved (i.e. atomically multifaceted), then Equations 7 and 8 show that the fastest and slowest etching surfaces (with respect to the $\langle 110 \rangle$ etch rates) will dominate over any intermediate orientation. If the ϕ value is exactly $5^\circ 48'$, the facets will have $\{771\}$ type indices; if ϕ is $6^\circ 44'$ the facets will be $\{661\}$. It may be objected that such high index faces are unlikely to occur, and that a $(77\bar{1})$ plane, for example, is possibly a stepped surface made up of unequal length segments of (110) and $(1\bar{1}\bar{1})$ planes. This objection is invalidated also by Equations 7 and 8: the complete domination of all intermediate orientations by the fastest (or slowest) etching face can only result in a single orientation facet.

3. This is to be expected. The etch rate anisotropy of (111) and $(\bar{1}\bar{1}\bar{1})$ wholly polar gallium arsenide, and other III-V surfaces is well known [8-10], and it is reasonable to expect some anisotropy in etching behaviour between partially-polar surfaces of opposite partial-polarity.

4. This assumption is a key factor: without this it is not possible for the initial formation of inclined surfaces to occur on each side of the junction, as shown in Fig. 11. The SEM micrographs of ridge and groove at the junction on adjacent cleavage faces is positive experimental evidence in support of this postulate.

Evidence for the occurrence of anisotropy of $[110]$ and $[\bar{1}10]$ misfit dislocations in junction regions has been given by Abrahams and Buiocchi [8], and more recently by Abrahams *et al* [12]. In this latter work it was shown that an asymmetry exists between orthogonal arrays of like-sign 60° misfit dislocations with $\mathbf{b} = \frac{1}{2} a_0 \langle 110 \rangle$. This could well produce differences in etching behaviour in the two orthogonal $\langle 110 \rangle$ directions along which the dislocations emerge at $\{110\}$ cleavage faces, since the earlier work [8] had indicated such differences for edge dislocations with $\mathbf{b} = \frac{1}{2} a_0 \langle 011 \rangle$.

It may not be necessary to evoke the presence of asymmetric misfit dislocations in order to account for an asymmetry in the junction etching behaviour. Fig. 10 shows that in the $\{110\}$ surface Ga and As atoms are triply bonded to the lattice; differences in electron-

affinity between the atoms will ensure that groups such as EFGH and E'F'G'H' act as (surface) local dipoles. Due to the asymmetry of the (110) and $(\bar{1}10)$ gallium arsenide surfaces these "dipoles" differ in orientation by π . If the {110} surfaces in Fig. 10 shown as ABCD and A'B'C'D' represent the junction regions then there is an electrochemical potential difference across the surfaces, opposed by the "dipoles" on one face, and reinforced by the antiparallel dipoles on the orthogonal face. It is possible that these differences may give rise to different etching attacks at the two junction regions.

3.4. Significance of the junction etch anisotropy

3.4.1. Double junctions

Although the majority of the results discussed in this work have been obtained by using the AB etch, the results shown in Figs. 2 and 3 indicate that the conventional junction etch behaves in a similar way, although reduced etch times and a different etch composition give very narrow bands. It is clear that the CEJ band, although it appears as two lines on Figs. 2 and 3, cannot be interpreted as either sufficient or necessary proof of the existence of a double junction.

3.4.2. Accurate junction location

The accurate optical location of a junction will usually be estimated from a series of measurements of the CEJ (band) position with respect to the layer surface. These measurements will normally be made on one cleavage face only, unless the readings are rechecked, perhaps at a later date, when a fresh cleave-and-etch may fortuitously be made on the orthogonal {110} face. In general, the measurements will be taken from the middle of the line (= etch band), and hence will have systematic positive or negative errors of one half of the band width from the true junction position. For an etch line of width $0.5 \mu\text{m}$ the error will thus be $\pm 0.25 \mu\text{m}$, and the sign of the error will depend on which face has been measured. Two sets of junction positions measured by optical cleave-and-etch of arbitrary {110} faces (J_0) and C—V profiling (J_p) for 106 different VPE sulphur-doped layers covering a layer thickness of 2 to $10 \mu\text{m}$ were compared [5], and the results are shown in Fig. 12.

The two peaks suggest that systematic equal-magnitude and opposite-sign errors are occurring in one or other of the measurements, and we believe that they demonstrate the expected



Figure 12 ($J_0 - J_p$) values for 106 layers.

cleave-and-etch errors. If the median value of the distribution is taken, there is a residual $0.3 \mu\text{m}$ discrepancy between the two different measurements, which probably reflects the arbitrary choice of junction position on the C—V profile, discussed in Section 1.

3.4.3. Detection of very thin layers

The presence of the AB etch bands can be used to indicate quickly the existence (or otherwise) of very thin ($< 0.2 \mu\text{m}$) layers, such as those obtained in molecular beam investigations [13]. Thus even if the layer thickness is less than that which can be resolved optically, the occurrence of an AB band on *one* {110} cleavage face is a clear indication of the existence of a junction. On the orthogonal {110} cleavage face the junction band width is of course limited by the layer thickness (e.g. specimen C Table II), whereas for the other cleavage face the band width is a function of the etching time.

Acknowledgements

The author wishes to thank many of his colleagues for innumerable useful discussions, particularly R. W. Bicknell, M. J. Cardwell, R. F. Peart and B. L. H. Wilson. He is indebted to

R. W. Bicknell for the suggestion which forms the basis of the final paragraph of Section 3.3., to N. F. Mott for helpful comments during various stages of the work, and to N. S. Griffin and G. V. Smith for skilful operation of the SEM. This paper incorporates work carried out under a C.V.D. contract and is published by permission of the Ministry of Defence (Procurement Executive). Acknowledgement is also made to the Plessey Company Limited for permission to publish.

References

1. P. A. SCHUMANN, JUN., *J. Electrochem. Soc.* **116** (1969) 409.
2. D. P. KENNEDY, P. C. MURLEY and W. KLEINFELDER, *I.B.M. J. Res. Develop.* **12** (1968) 399.
3. M. P. ALBERT and J. F. COMBS, *J. Electrochem. Soc.* **109** (1962) 709.
4. G. H. SCHWUTKE and H. RUPPRECHT, *J. Appl. Phys.* **37** (1966) 167.
5. R. F. PEART and M. J. CÅRDWELL, unpublished results (1971-72).
6. R. W. BICKNELL, to be published.
7. M. S. ABRAHAMS and C. J. BUIOCCHI, *J. Appl. Phys.* **37** (1966) 1973.
8. *Idem, ibid* **36** (1965) 2855.
9. H. C. GATOS and M. C. LEVINE, *J. Electrochem. Soc.* **107** (1960) 427.
10. *Idem, ibid* **107** (1960) 433.
11. A. M. HUBER and G. CHAMPIER, 3rd International Symposium on Gallium Arsenide, Aachen (1970) Paper 13, p. 118.
12. M. S. ABRAHAMS, J. BLANC and C. J. BUIOCCHI, *Appl. Phys. Letters* **21** (1972) 185.
13. J. R. ARTHUR and J. J. LE PORE, *J. Vac. Sci. Tech.* **6** (1969) 545.

Received 17 September and accepted 5 December 1973.